

Lifetime Differences and CP Violation Parameters of Neutral B Mesons at the Next-to-Leading Order in QCD

M. Ciuchini^a, E. Franco^b, V. Lubicz^a,
F. Mescia^c, and C. Tarantino^a

^a Dip. di Fisica, Univ. di Roma Tre and INFN, Sezione di Roma III,
Via della Vasca Navale 84, I-00146 Rome, Italy

^b Dip. di Fisica, Univ. di Roma "La Sapienza" and INFN, Sezione di Roma,
P.le A. Moro 2, I-00185 Rome, Italy

^c Dept. of Physics and Astronomy, Univ. of Southampton,
Highfield, Southampton, SO17 1BJ, U.K.

Abstract

We compute the next-to-leading order QCD corrections to the off-diagonal elements of the decay-width matrix entering the neutral B-meson oscillations. From this calculation the width differences and the CP violation parameters (q/p) of B_d and B_s mesons are estimated, including the complete $O(\alpha_s)$ QCD corrections and the $1/m_b$ contributions. For the width difference $\Delta\Gamma_s$ we agree with previous results. By using the lattice determinations of the relevant hadronic matrix elements we obtain the theoretical predictions $\Delta\Gamma_d/\Gamma_d = (2.42 \pm 0.59) \cdot 10^{-3}$ and $\Delta\Gamma_s/\Gamma_s = (7.4 \pm 2.4) \cdot 10^{-2}$. For the CP violation parameters, we find $|j(q/p)_d| = (2.96 \pm 0.67) \cdot 10^{-4}$ and $|j(q/p)_s| = (1.28 \pm 0.27) \cdot 10^{-5}$. These predictions are compatible with the experimental measurements which, however, suffer at present from large uncertainties.

1 Introduction

B physics plays an important role to test and improve our understanding of the Standard Model (SM). By exploiting the production of B_d mesons with a large boost, experiments such as BaBar and Belle can provide accurate measurements of the decay time distributions and hence valuable information for the B_d -meson lifetimes, CP violation and mixing parameters. The production of B_s , on the other hand, is out of the reach of the B-factories and improved measurements of the related physical observables will come from the Run II at Tevatron and from the LHC. Recently, the measurement of the mass difference m_d , which controls the frequency of B_d oscillations, has been further improved. The world average is now $m_d = (0.502 \pm 0.006) \text{ ps}^{-1}$ [1]. For m_s and for the width differences Γ_d and Γ_s , instead, only weak limits exist at present. Theoretically, the width differences are suppressed by a factor m_b^2/m_t^2 with respect to the corresponding mass differences. In addition, Γ_s is predicted to be larger than Γ_d , the latter being doubly Cabibbo-suppressed.

The present world average for the width difference of B_s mesons is [1]

$$\Gamma_s/\Gamma_s = 0.07^{+0.09}_{-0.07}; \quad (1)$$

where the constraint $\Gamma(B_s) = \Gamma(B_d)$ has been used. Concerning the B_d system, a preliminary result for Γ_d has been recently presented by the BaBar collaboration [2]. The experimental result reads¹

$$\Gamma_d/\Gamma_d = 0.008 \pm 0.037 (\text{stat.}) \pm 0.018 (\text{syst.}); \quad (2)$$

In ref. [2], a preliminary measurement of the parameter $j(\text{CP})_d$, which denotes the amount of CP violation in the mixing, is also presented

$$j(\text{CP})_d - 1 = 0.029 \pm 0.013 (\text{stat.}) \pm 0.011 (\text{syst.}); \quad (3)$$

In the SM, the CP violation parameters $j(\text{CP})_d - 1$ and $j(\text{CP})_s - 1$ are suppressed, with respect to the width differences, by a factor m_c^2/m_b^2 . Moreover, $j(\text{CP})_s - 1$ has an additional suppression factor $\sin^2 \theta$ (where θ is the sine of the Cabibbo angle) with respect to $j(\text{CP})_d - 1$.

The phenomenology of $B_q - \bar{B}_q$ oscillations is described in terms of a 2×2 effective Hamiltonian matrix, $M^q - i\Gamma^q/2$. The b-quark mass, being large compared to m_{QCD} , allows to apply an operator product expansion (OPE) to the calculation of the decay-width matrix Γ^q [4, 5]. In the case of the off-diagonal matrix elements, which the observables Γ_d and Γ_s are related to, the leading term in this expansion is represented by the so-called "spectator effect" contributions.

Recently, spectator effects have been computed at $O(1/m_s)$ and $O(1/m_{QCD} - m_b)$ for the B -meson and b -lifetimes [6]–[9] and for the Cabibbo-favoured transition $(b \rightarrow cc)$ contributing to Γ_s [10, 11]. In the case of Γ_d , the complete set of the $m_{QCD} - m_b$ contributions has

¹Note that the definition of Γ_d used in this paper has an opposite sign with respect to one used in the BaBar paper. In addition, the measurement itself has a sign ambiguity that can be removed only by measuring the sign of $\cos 2\theta$, where θ is the phase of the mixing. This sign is not measured yet but it is known to be positive in the SM, see e.g. [3].

been presented in [12], but the QCD next-to-leading order (NLO) corrections have been only estimated in that paper in the limit of vanishing charm quark mass, using the results of [11].

The main result of this paper is the calculation of NLO QCD corrections to \bar{s}_{21}^d including the contributions from a non-vanishing charm quark mass. Our results for the NLO Wilson coefficients of \bar{s}_{21}^s agree with ref. [11] and in addition we have computed the Cabibbo-suppressed contributions. We have also checked the computation of the $\bar{Q}_{CD} = m_b$ corrections to \bar{s}_{21}^s and \bar{s}_{21}^d at the LO in QCD and the results agree with refs. [10, 12]. Finally, we have computed the matching between the QCD and HQET $B = 2$ operators at the NLO in QCD and found agreement with the results presented in ref. [13]. As phenomenological applications of our calculations, by using the lattice determinations of the relevant hadronic matrix elements [13], we estimate the width differences $\Delta\Gamma_d$, $\Delta\Gamma_s$ and the CP violation parameters $(\bar{q}q)_d$ and $(\bar{q}q)_s$.

The inclusion of NLO corrections is important in order to match the scale and scheme dependence of the renormalized operators entering the OPE with that of the Wilson coefficients, thus reducing the theoretical uncertainties. In addition, the NLO corrections are found to be generally large. Taking into account the finite value of the charm quark mass is also an important issue for a proper NLO estimate of $\Delta\Gamma_d$ and of the CP violation parameters $j(\bar{q}q)_d$ and $j(\bar{q}q)_s$. In the limit $m_c \rightarrow 0$, $\Delta\Gamma_d$ becomes independent of the phase of the mixing amplitude (2β in the SM) and CP is not violated in the mixing, i.e. $j(\bar{q}q)_d$ and $j(\bar{q}q)_s$ are simply equal to one [14]. Therefore, the dependence on the mixing phase as well as the CP violating terms disappear from the NLO corrections in the vanishing charm mass limit.

Our theoretical estimates of the width differences, obtained by using the lattice determinations of the relevant hadronic matrix elements [13], are

$$\Delta\Gamma_s = \Delta\Gamma_s = (7.4 \pm 2.4) \cdot 10^{-2}; \quad \Delta\Gamma_d = \Delta\Gamma_d = (2.42 \pm 0.59) \cdot 10^{-3}. \quad (4)$$

These results can only be compared at present with the experimental determinations given in eqs. (1) and (2). The predictions are consistent with the measured values but, given the large experimental uncertainties, it is certainly premature to draw any conclusion. Our estimates are accurate at the NLO in $\Delta\Gamma_s$ for the leading term in the $1/m_b$ expansion and at the LO for the first power-correction.

It is interesting to consider also the estimate of the ratio $\Delta\Gamma_d = \Delta\Gamma_s$, for which we obtain the prediction

$$\Delta\Gamma_d = \Delta\Gamma_s = (3.2 \pm 0.8) \cdot 10^{-2}. \quad (5)$$

In this ratio the uncertainties coming from higher orders of QCD and $\bar{Q}_{CD} = m_b$ corrections, as well as from the non perturbative estimates of the hadronic matrix elements, cancel out to some extent.

Finally, our predictions for the CP violation parameters are

$$j(\bar{q}q)_d = 1 = (2.96 \pm 0.67) \cdot 10^{-4}; \quad j(\bar{q}q)_s = 1 = (1.28 \pm 0.27) \cdot 10^{-5}. \quad (6)$$

The value of $j(\bar{q}q)_d$ can be compared with the preliminary experimental determination given in eq. (3). Improved measurements are certainly needed to make this comparison more significant.

We conclude this section by presenting the plan of this paper. In sect. 2 we review the basic formalism of the $B_q - \bar{B}_q$ mixing, introducing all the physical quantities we are interested in. The details of the NLO calculation are presented in sect. 3, along with the calculation of the $QCD \Rightarrow m_b$ correction. In sect. 4 we present the theoretical predictions for the observables under consideration in both the $B_d - \bar{B}_d$ and $B_s - \bar{B}_s$ systems. Finally, the analytical expressions for the matching coefficient functions are given in appendix A, while detailed definitions of the renormalization schemes used in the calculation and results for the matching between QCD and HQET operators can be found in appendix B.

2 $B_q - \bar{B}_q$ Basic Formalism

The neutral B_d and B_s mesons mix with their antiparticles leading to oscillations between the mass eigenstates. The time evolution of the neutral mesons doublet is described by a Schroedinger equation with an effective 2×2 Hamiltonian

$$i \frac{d}{dt} \begin{pmatrix} B_q \\ \bar{B}_q \end{pmatrix} = \begin{pmatrix} M_{11}^q & M_{21}^q \\ M_{21}^q & M_{11}^q \end{pmatrix} \begin{pmatrix} B_q \\ \bar{B}_q \end{pmatrix} : \quad (7)$$

The mass difference m_q and the width difference Γ_q are defined as

$$m_q = m_H^q - m_L^q; \quad \Gamma_q = \Gamma_L^q - \Gamma_H^q; \quad (8)$$

where H and L denote the Hamiltonian eigenstates with the heaviest and lightest mass eigenvalue respectively. These states can be written as

$$|B_q^{L,H}\rangle = \frac{1}{\sqrt{1 + |(\phi\bar{p})_q|^2}} \left(|B_q\rangle - (\phi\bar{p})_q |\bar{B}_q\rangle \right) : \quad (9)$$

The phase of $(\phi\bar{p})_q$ depends on the phase convention of the B states and hence it is not measurable by itself. In this paper, we are interested in $|(\phi\bar{p})_q|$ only.

Theoretically, the experimental observables m_q , Γ_q and $|(\phi\bar{p})_q|$ are related to M_{21}^q and M_{11}^q in eq. (7) as follows²

$$\begin{aligned} (m_q)^2 - \frac{1}{4}(\Gamma_q)^2 &= 4|M_{21}^q|^2 - |(\phi\bar{p})_q|^2; \\ m_q - \Gamma_q &= 4\text{Re}(M_{21}^q); \quad (\phi\bar{p})_q = \frac{2M_{21}^q - i\Gamma_q}{2M_{21}^q - i\Gamma_q} : \end{aligned} \quad (10)$$

In the $B_d - \bar{B}_d$ and $B_s - \bar{B}_s$ systems, the ratio $\frac{M_{21}^q}{M_{11}^q}$ is of $O((m_b^2 - m_t^2)^{-1}) \sim 10^{-3}$. Therefore, by neglecting terms of $O((m_b^4 - m_t^4)^{-1})$, eq. (10) can be simply written as

$$m_q = 2|M_{21}^q|; \quad \Gamma_q = 2|M_{21}^q| \text{Re} \left(\frac{(\phi\bar{p})_q}{M_{21}^q} \right); \quad (\phi\bar{p})_q = 1 + \frac{1}{2} \text{Im} \left(\frac{(\phi\bar{p})_q}{M_{21}^q} \right) : \quad (11)$$

²For more information about the basic definitions in the $B_d - \bar{B}_d$ - and $B_s - \bar{B}_s$ -mixing, see for instance [1] and references therein.

The matrix elements M_{21}^q and \bar{M}_{21}^q are related to the dispersive and the absorptive parts of the $B = 2$ transitions respectively. In the SM, these transitions are the result of second-order charged weak interactions involving the well-known box diagrams.

The quantity M_{21}^q has been computed, at the NLO in QCD, in ref. [15] and it is given by

$$M_{21}^q = \frac{G_F^2 M_W^2}{(4\pi)^2 (2M_{B_q})} (V_{tb}V_{tq})^2 S_0(x_t) h\bar{B}_q j(b_i q_i)_{V-A} (b_j q_j)_{V-A} \mathcal{B}_q; \quad (12)$$

where $x_t = m_t^2/M_W^2$, M_{B_q} is the QCD correction factor and S_0 is the Inami-Lim function. Here and in the following we use the notation $(qq)_{V-A} = q(1-\gamma_5)q$ and $(qq)_{S-P} = q(1+\gamma_5)q$. A sum over repeated colour indices is always understood.

The matrix element \bar{M}_{21}^q can be written as

$$\bar{M}_{21}^q = \frac{1}{2M_{B_q}} \text{Disc} \bar{B}_q j \int_0^1 dx T H_{\text{eff}}^{B=1}(x) H_{\text{eff}}^{B=1}(0) \mathcal{B}_q; \quad (13)$$

where "Disc" picks up the discontinuities across the physical cut in the time-ordered product of the effective Hamiltonians.

The $B = 1$ effective Hamiltonian relevant to $b \rightarrow d$ and $b \rightarrow s$ transitions is

$$H_{\text{eff}}^{B=1} = \frac{G_F}{2} V_{cb}V_{ud} (C_1 Q_1 + C_2 Q_2) + V_{cb}V_{cd} (C_1 Q_1^c + C_2 Q_2^c) + (c \leftrightarrow u) \\ + \sum_{i=3}^6 V_{tb}V_{td} C_i Q_i + C_{8G} Q_{8G} + d \rightarrow s + \text{h.c.}; \quad (14)$$

The C_i are the $B = 1$ Wilson coefficients, known at the NLO in perturbation theory [16]–[18], and the operators Q_i are defined as

$$\begin{aligned} Q_1 &= (b_i c_j)_{V-A} (u_j d_i)_{V-A}; & Q_2 &= (b_i c_i)_{V-A} (u_j d_j)_{V-A}; \\ Q_1^c &= (b_i c_j)_{V-A} (c_j d_i)_{V-A}; & Q_2^c &= (b_i c_i)_{V-A} (c_j d_j)_{V-A}; \\ Q_3 &= (b_i d_i)_{V-A} \sum_q (q_j q_j)_{V-A}; & Q_4 &= (b_i d_j)_{V-A} \sum_q (q_j q_i)_{V-A}; \\ Q_5 &= (b_i d_i)_{V-A} \sum_q (q_j q_j)_{V+A}; & Q_6 &= (b_i d_j)_{V-A} \sum_q (q_j q_i)_{V+A}; \\ Q_{8G} &= \frac{g_s}{8} m_b b_i (1-\gamma_5) t_{ij}^a d_j G^a; \end{aligned} \quad (15)$$

Due to the large mass of the b quark, the time-ordered product in eq. (13) can be expanded in a sum of local operators of increasing dimension [4, 5]. Up to order $1/m_b$, this expansion reads

$$\bar{M}_{21}^q = \frac{G_F^2 m_b^2}{24 M_{B_q}} h c_1^q(\mu) h\bar{B}_q \mathcal{D}_1^q(\mu) \mathcal{B}_q + c_2^q(\mu) h\bar{B}_q \mathcal{D}_2^q(\mu) \mathcal{B}_q + \sum_{i=1}^4 \bar{M}_{21}^{q,i}; \quad (16)$$

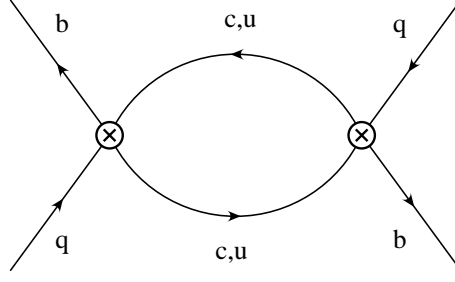


Figure 1: Feynman diagram contributing to \bar{q}_{21} at the LO in QCD.

where

$$O_1^q = (b_i q_i)_{V-A} (b_j q_j)_{V-A}; \quad O_2^q = (b_i q_i)_{S-P} (b_j q_j)_{S-P}; \quad (17)$$

and $\bar{q}_{1=m}$ denotes the sub-leading $1=m_b$ corrections. Thus, the OPE of \bar{q}_{21} at the leading order is expressed in terms of only two local four-fermion operators, O_1^q and O_2^q .

In terms of the CKM matrix elements $V_{cb}V_{cq}$ and $V_{tb}V_{tq}$ (the latter regulates the M_{21}^q contribution), the Wilson coefficients c_i^q and the $\bar{q}_{1=m_b}$ in eq. (16) can be written as

$$\begin{aligned} c_1^q &= (V_{tb}V_{tq})^2 D_i^{uu} + 2V_{cb}V_{cq}V_{tb}V_{tq} (D_i^{uu} - D_i^{cu}) + (V_{cb}V_{cq})^2 (D_i^{cc} + D_i^{uu} - 2D_i^{cu}); \\ \bar{q}_{1=m}^q &= (V_{tb}V_{tq})^2 \bar{q}_{1=m}^{uuq} + 2V_{cb}V_{cq}V_{tb}V_{tq} \bar{q}_{1=m}^{uuq} - \bar{q}_{1=m}^{cuq} + (V_{cb}V_{cq})^2 \bar{q}_{1=m}^{ccq} + \bar{q}_{1=m}^{uuq} - 2\bar{q}_{1=m}^{cuq} \end{aligned} \quad (18)$$

where the labels cc; cu and uu denote the intermediate quark pair contributing to \bar{q}_{21}^q , see the diagram in fig. 1. The unitarity of the CKM matrix has been used to drop out $V_{ub}V_{uq} = -V_{cb}V_{cq} - V_{tb}V_{tq}$.

In this paper, we compute the QCD NLO corrections to $D_i^{cc}; D_i^{cu}; D_i^{uu}$ taking into account the finite value of the charm quark mass. Our results are collected in appendix A. The results for D_i^{cc} are in agreement with a previous calculation [11]. The functions $D_i^{cu}; D_i^{uu}$ have been previously estimated [12] taking the limit of a massless charm quark of D_i^{cc} . As stressed in the introduction, this approximation is not fully satisfactory, in particular if one wants to investigate the dependence on the phase of the mixing in $\theta_d = \theta$ and the β - γ parameters.

As far as the $1=m$ contributions are concerned, $\bar{q}_{1=m}^{ccq}$ and $\bar{q}_{1=m}^{cuq}, \bar{q}_{1=m}^{uuq}$ in eq. (18) have been calculated in [10] and [12] respectively. We have repeated the calculation by expanding in $1=m_b$ the relevant Feynman diagrams and found agreement with the previous results.

3 Calculation of the Wilson coefficients for \bar{q}_{21}^q

In this section, we discuss the basic ingredients of the calculation of the NLO QCD corrections to \bar{q}_{21}^q , at the leading power in $1=m_b$, and of the calculation of the $1=m_b$ corrections at the LO in QCD. We refer the interested reader to refs. [6, 8] for further details on the NLO calculation.

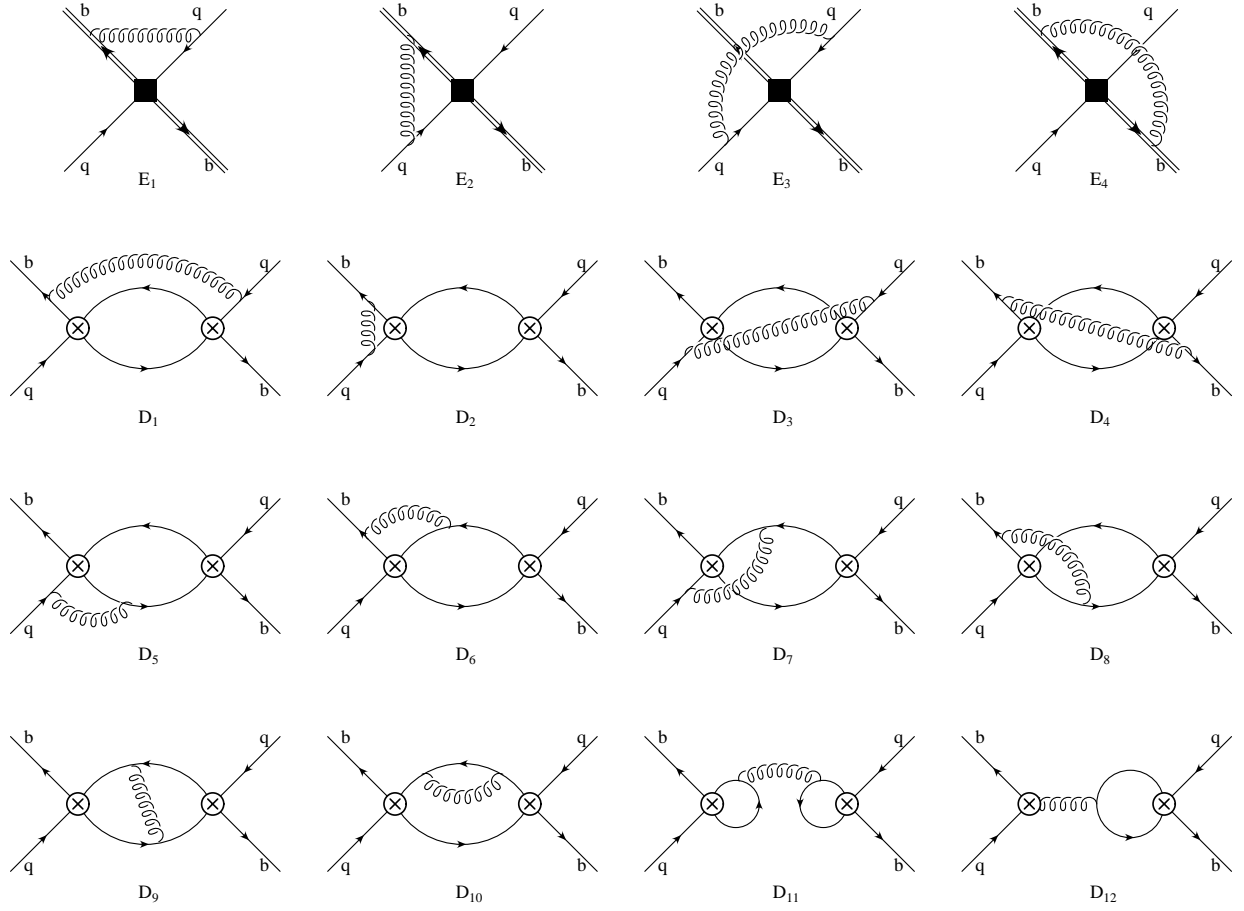


Figure 2: Feynman diagrams which contribute at the NLO to the matrix element of the transition operator T , both in the full theory (D_i) and in the effective theory (E_i). The diagrams obtained from $E_1; E_2; D_1; D_2; D_5; D_6; D_7; D_8; D_{10}$ and D_{12} by a 180° rotation (keeping fixed the flavour of the internal lines), as well as those containing the self-energy one-loop corrections to the external fields are not shown.

3.1 NLO QCD corrections at the leading order in $1=m_b$

Although at the leading order in $1=m_b$ the heavy quark expansion of the width difference could be expressed directly in terms of QCD operators, we found it easier to perform first the expansion in terms of HQET operators and then translating the results into QCD, once IR divergences are canceled out.

In order to compute the Wilson coefficients of the $B = 2$ operators at the NLO, we have evaluated in QCD the imaginary part of the diagrams D_i shown in fig. 2 (full theory) and in the HQET the diagrams E_i (effective theory). The external quark states have been taken on-shell and all quark masses, except m_b and m_c , have been neglected. More specially, we have chosen the heavy quark momenta $p_b^2 = m_b^2$ in QCD and $k_b = 0$ in the HQET while, for the external light quarks, $p_q = 0$ in both cases. We have performed the calculation in a generic covariant gauge, in order to check the gauge independence of

the final results. Two-loop integrals have been reduced to a set of independent master integrals by using the TARCER package [19].

IR and UV divergences have been regularized by D -dimensional regularization with anticommuting γ_5 (NDR). As discussed in detail in ref. [6], in the presence of dimensionally-regularized IR divergences the matching must be consistently performed in D dimensions, including the contribution of (renormalized) evanescent operators [20]. All the evanescent operators entering the matching procedure are collected in appendix B.

As a check of the perturbative calculation, we have verified that our results for the Wilson coefficients satisfy the following requirements:

gauge invariance: the coefficient functions in the $\overline{\text{MS}}$ scheme are explicitly gauge-invariant. The same is true for the full and the effective amplitudes separately;

renormalization-scale dependence: the coefficient functions have the correct logarithmic scale dependence as predicted by the LO anomalous dimensions of the $B = 2$ and $B = 1$ operators;

renormalization-scheme dependence: we performed the calculation in two different NDR- $\overline{\text{MS}}$ schemes for the $B = 2$ operators (see appendix B and refs. [11, 21] for a detailed definition of these schemes) and verified that the NLO Wilson coefficients obtained in the two cases are related by the appropriate matching matrix;

IR divergences: the coefficient functions are infrared finite;

IR regularization: in the limit $m_c \rightarrow 0$, we have also checked that a calculation using the gluon mass as IR regulator gives the same results. In this case, the matrix elements of the renormalized evanescent operators vanish and hence these operators do not give contribution in the matching procedure;

comparison with the results in [11]: our results for D_i^{cc} defined in eq. (18) and given in appendix A agree with those obtained in ref. [11].

The $B = 2$ effective theory is derived from the double insertion of the $B = 1$ effective Hamiltonian. Therefore, the coefficient functions $D_k^{\text{cc}}, D_k^{\text{cu}}$ and D_k^{uu} of the $B = 2$ effective theory depend quadratically on the coefficient functions C_i of the $B = 1$ effective Hamiltonian. The dependence on the renormalization scheme and on the scale μ_1 of the $B = 1$ operators actually cancels order by order in perturbation theory against the corresponding dependence of the $B = 1$ Wilson coefficients C_i . Therefore, the coefficient functions c_k^{q} only depend on the renormalization scheme and on the scale μ_2 of the $B = 2$ operators.

The analytical expressions of the Wilson coefficients are collected in appendix A. For illustrative purposes, the corresponding numerical values, at the reference scales $\mu_1 = \mu_2 = m_b$, are presented in table 1. In this table, the LO and NLO coefficients are shown together with the pure $O(\alpha_s)$ contribution, both in the case of a finite charm quark mass and in the charm massless limit³. The NLO coefficients refer to the QCD operators renormalized

³Note that, in what we call the pure $O(\alpha_s)$ contribution in table 1, the NLO corrections to the $B = 1$ Wilson coefficients are not included. For this reason, the NLO results in the table 1 differ from the sums of the LO coefficients and the pure $O(\alpha_s)$ contributions.

	LO	$O(s)$	NLO	$O(s)$	NLO
	$s m_c = 0$				
D_1^{uu}	0.260	-0.123	0.174	-0.123	0.174
$D_1^{uu} - D_1^{cu}$	0.103	0	0.105	-0.034	0.072
$D_1^{cc} + D_1^{uu} - 2D_1^{cu}$	0.004	0	0.004	-0.005	-0.001
D_2^{uu}	-1.56	0.44	-1.00	0.44	-1.00
$D_2^{uu} - D_2^{cu}$	-0.035	0	-0.033	0.012	-0.022
$D_2^{cc} + D_2^{uu} - 2D_2^{cu}$	0.016	0	0.015	-0.014	0.001

Table 1: Values of the Wilson coefficients defined in eq. (18) computed at the reference scales $\mu_1 = \mu_2 = m_b = 4.75 \text{ GeV}$. The LO (first column) and NLO (third and fifth column) coefficients are shown together with the pure $O(s)$ contribution (second and fourth column). The results given in the second and third column are those obtained by neglecting the $O(s m_c)$ corrections.

in the $\overline{\text{NDR}}\text{-}\overline{\text{MS}}$ scheme of ref. [11]. In order to obtain the numerical results we used the central values of the input parameters given in table 2.

By looking at the results shown in table 1, we see that the NLO corrections are large and the effect of charm contributions is crucial to estimate accurately all the terms in eq. (18).

3.2 $1=m_b$ Corrections to \bar{q}_{21} at the LO in QCD

In order to compute the $1=m_b$ correction at the LO in QCD, the imaginary part of the diagrams in fig. 1 have been evaluated between on-shell quark states and expanded in the quark momenta⁴. The result of the full theory has been then matched at $O(1=m_b)$ onto the following independent set of QCD operators,

$$\begin{aligned}
 R_1^q &= \frac{m_q}{m_b} (\bar{b}_i q_i)_{S-P} (\bar{b}_j q_j)_{S+P}; & R_2^q &= \frac{1}{m_b^2} (\bar{b}_i D_{\mu} (1-\gamma_5) D_{\mu} q_i) (\bar{b}_j (1-\gamma_5) q_j); \\
 R_3^q &= \frac{1}{m_b^2} (\bar{b}_i D_{\mu} (1-\gamma_5) D_{\mu} q_i) (\bar{b}_j (1-\gamma_5) q_j); & R_4^q &= \frac{1}{m_b} (\bar{b}_i (1-\gamma_5) i D_{\mu} q_i) (\bar{b}_j (1-\gamma_5) q_j);
 \end{aligned} \tag{19}$$

⁴In the heavy quark expansion we consider the strange quark mass of $O(\Lambda_{\text{QCD}})$, whereas m_u and m_d are neglected.

Since derivatives acting on fields scale as m_b , the above operators are manifestly of order $1/m_b$. The results for the $1/m_b$ terms defined in eq. (18) read

$$\begin{aligned}
\frac{ccq}{1=m} &= \frac{p}{1-4z} ((1+2z) [K_2 (hR_2^q i + 2hR_4^q i) - 2K_1 (hR_1^q i + hR_2^q i)] \\
&\quad - \frac{12z^2}{1-4z} [K_1 (hR_2^q i + 2hR_3^q i) + 2K_2 hR_3^q i]) ; \\
\frac{cuq}{1=m} &= (1-z)^2 ((1+2z) [K_2 (hR_2^q i + 2hR_4^q i) - 2K_1 (hR_1^q i + hR_2^q i)] \\
&\quad - \frac{6z^2}{(1-z)} [K_1 (hR_2^q i + 2hR_3^q i) + 2K_2 hR_3^q i]) ; \\
\frac{uuq}{1=m} &= [K_2 (hR_2^q i + 2hR_4^q i) - 2K_1 (hR_1^q i + hR_2^q i)] ;
\end{aligned} \tag{20}$$

where K_1 and K_2 are related to the $B = 1$ coefficients, $K_1 = 3C_1^2 + 2C_1 C_2$ and $K_2 = C_2^2$, and $z = (m_c/m_b)^2$. Our results agree with previous calculations [10, 12]⁵.

4 Width differences and CP violation parameters in $B_q - \bar{B}_q$ mixing

In this section we present the theoretical estimates for the quantities of interest in this paper: the width differences $\Delta\Gamma_d$ and $\Delta\Gamma_s$ and the CP violation parameters $j(\text{CP})_d$ and $j(\text{CP})_s$.

Our estimates neglect terms of $O((\frac{2}{s})$, $O(s(\mu_{CD}/m_b))$ and $O((\mu_{CD}/m_b)^2)$, whereas the charm quark mass contributions have been fully taken into account. For the relevant hadronic matrix elements we have used the lattice determination of ref. [13].

In eq. (11), the width difference $\Delta\Gamma_q$ and the parameter $j(\text{CP})_q$ for neutral B mesons are expressed in terms of the real and the imaginary part of $\frac{q}{21} = M_{21}^q$ respectively. Taking into account the expressions obtained in eq. (12) for M_{21}^q and eqs. (16)–(18) for $\frac{q}{21}$, we can write

$$\begin{aligned}
\Delta\Gamma_q &= \frac{m_q K}{2\text{Re}(\text{Im}(\frac{q}{21}))} \\
&\quad \times \left[\text{Re}(\frac{q}{21}) + \frac{\cos 2\theta_q}{R_{tq}^2} (\text{Re}(\frac{ccq}{1=m} + \text{Re}(\frac{uuq}{1=m}) - 2\text{Re}(\frac{cuq}{1=m})) - 2\frac{\cos \theta_q}{R_{tq}} (\text{Re}(\frac{uuq}{1=m}) - \text{Re}(\frac{cuq}{1=m}))) \right. \\
&\quad \left. + \frac{\text{Im}(\frac{uuq}{1=m}) + \frac{\cos 2\theta_q}{R_{tq}^2} (\text{Im}(\frac{ccq}{1=m}) + \text{Im}(\frac{uuq}{1=m}) - 2\text{Im}(\frac{cuq}{1=m})) - 2\frac{\sin \theta_q}{R_{tq}} (\text{Im}(\frac{uuq}{1=m}) - \text{Im}(\frac{cuq}{1=m}))}{\text{Re}(\frac{q}{21})} \right] ; \tag{21}
\end{aligned}$$

$$\frac{j(\text{CP})_q}{\text{Re}(\frac{q}{21})} = \frac{\text{Im}(\frac{q}{21})}{2\text{Re}(\text{Im}(\frac{q}{21}))}$$

⁵For the reader's benefit, we observe that the expression of $\frac{ccq}{1=m}$ in eq. (49) of ref. [12] has been expanded up to $O(z^3)$.

$$\begin{aligned}
& \mathcal{O}^X_{i=1/2} \left[\overline{hB}_q \mathcal{P}^q_i \mathcal{P}_{qi} - \frac{\sin 2\varphi_q}{R_{tq}^2} (\mathcal{D}^{cc}_i + \mathcal{D}^{uu}_i - 2\mathcal{D}^{cu}_i) - 2 \frac{\sin \varphi_q}{R_{tq}} (\mathcal{D}^{uu}_i - \mathcal{D}^{cu}_i) \right] \\
& + \frac{\sin 2\varphi_q}{R_{tq}^2} \left[\mathcal{D}^{cc}_{1=m} + \mathcal{D}^{uu}_{1=m} - 2\mathcal{D}^{cu}_{1=m} \right] - 2 \frac{\sin \varphi_q}{R_{tq}} \left[\mathcal{D}^{uu}_{1=m} - \mathcal{D}^{cu}_{1=m} \right] : \quad (22)
\end{aligned}$$

The two operators entering these expansions at the leading order, \mathcal{O}^q_1 and \mathcal{O}^q_2 , are defined in eq. (17). The coefficient K is given by $K = 4 m_b^2 = (3M_W^2 - 4S_0(x_t))$. In addition we have used

$$V_{cb}V_{cq} = (V_{tb}V_{tq}) = e^{i\varphi_q} R_{tq} : \quad (23)$$

φ_d and R_{td} are the usual angle and the side R_t of the unitarity triangle respectively, whereas φ_s and R_{ts} parameterize the Cabibbo-suppressed contributions to the B_s system. For completeness, we give their expansion in terms of the parameters of CKM matrix, up to and including $\mathcal{O}(\lambda^4)$ terms. They read

$$\begin{aligned}
R_{td} &= \frac{\varphi_q}{(1 - \lambda^2)^2 + \lambda^2}; \quad \sin \varphi_d = \lambda R_{td}; \\
R_{ts} &= 1 + \lambda^2 + \frac{1}{2} \lambda^4 (2 + \lambda^2); \quad \sin \varphi_s = \lambda^2 [1 + \lambda^2 (1 - \lambda^2)]: \quad (24)
\end{aligned}$$

The Cabibbo-suppressed contributions are practically irrelevant for φ_s so that, to an excellent approximation, one can put $\varphi_s = 0$ and $R_{ts} = 1$ in eq. (21) to obtain

$$\mathcal{B}_s = \frac{m_s K}{\overline{hB}_s \mathcal{P}^s_1 \mathcal{P}_{s1}} \mathcal{O}^X_{i=1/2} \left[\overline{hB}_s \mathcal{P}^s_i \mathcal{P}_{si} \mathcal{D}^{cc}_i + \mathcal{D}^{cc}_s + \mathcal{O}(\lambda^2) \right] : \quad (25)$$

The contributions neglected in the previous equation, however, give rise to the CP violation effects in the $B_s - \overline{B}_s$ mixing, which are accounted for by the deviation of the parameter $j(q-p)_s$ from unity. Using $\varphi_s = 0$ and $R_{ts} = 1$ in eq. (22) gives in fact $j(q-p)_s = 1$.

For the matrix elements entering our calculation (see eqs. (17) and (19)), we use the following parameterization

$$\begin{aligned}
\overline{hB}_q \mathcal{P}^q_1 \mathcal{P}_{q1} &= \frac{8}{3} f_{B_q}^2 M_{B_q}^2 B_1^q; & \overline{hB}_q \mathcal{P}^q_2 \mathcal{P}_{q2} &= \frac{5}{3} \frac{f_{B_q}^2 M_{B_q}^4}{(m_b + m_q)^2} B_2^q; \\
\overline{hB}_q \mathcal{P}^q_3 \mathcal{P}_{q3} &= \frac{7}{3} \frac{m_q}{m_b} f_{B_q}^2 M_{B_q}^2 B_{R1}^q; & \overline{hB}_q \mathcal{P}^q_4 \mathcal{P}_{q4} &= \frac{2}{3} f_{B_q}^2 M_{B_q}^2 \frac{M_{B_q}^2}{m_b^2} (1 - B_{R2}^q); \\
\overline{hB}_q \mathcal{P}^q_5 \mathcal{P}_{q5} &= \frac{7}{6} f_{B_q}^2 M_{B_q}^2 \frac{M_{B_q}^2}{m_b^2} (1 - B_{R3}^q); & \overline{hB}_q \mathcal{P}^q_6 \mathcal{P}_{q6} &= f_{B_q}^2 M_{B_q}^2 \frac{M_{B_q}^2}{m_b^2} (1 - B_{R4}^q) : \quad (26)
\end{aligned}$$

Among these B -parameters, B_1^q and B_2^q are the most widely studied and well known in lattice QCD [13], [23]–[29].⁶ In this paper we use the results of ref. [13], in which the complete set of $B = 2$, dimension-six, four-fermion operators has been determined in the quenched approximation of QCD. For B_1^q and B_2^q , the results of [13] are in very

⁶For estimates of these matrix elements based on QCD sum rules, see refs. [30]–[32].

good agreement with those obtained in [24, 25] by using the lattice NRQCD approach. In addition, it has been shown in refs. [28, 29] that the effect of the quenching approximation for these quantities is practically irrelevant. Thus, the systematic uncertainties in the present lattice estimates of B_1^q and B_2^q are quite under control.

To our knowledge, the matrix elements of the operators R_i^q defined in eq. (26), entering the $1=m_b$ corrections, have been only estimated so far in the VSA. Using the complete set of operator matrix elements calculated in [13], however, two of the four independent parameters $B_{R_i}^q$ can be also evaluated. Besides the operators $O_{1,2}^q$, the complete basis studied in [13] includes

$$O_3^q = (\bar{b}_i q_j)_{S-P} (b_j q_i)_{S-P}; \quad O_4^q = (\bar{b}_i q_i)_{S-P} (b_j q_j)_{S+P}; \quad O_5^q = (\bar{b}_i q_j)_{S-P} (b_j q_i)_{S+P}; \quad (27)$$

whose matrix elements are parametrized as

$$\begin{aligned} \langle \bar{B}_q | \bar{\psi} \gamma_3 \psi | B_q \rangle &= \frac{1}{3} \frac{m_{B_q}}{m_b + m_q} m_{B_q}^2 f_{B_q}^2 B_3^q; \\ \langle \bar{B}_q | \bar{\psi} \gamma_4 \psi | B_q \rangle &= 2 \frac{m_{B_q}}{m_b + m_q} m_{B_q}^2 f_{B_q}^2 B_4^q; \\ \langle \bar{B}_q | \bar{\psi} \gamma_5 \psi | B_q \rangle &= \frac{2}{3} \frac{m_{B_q}}{m_b + m_q} m_{B_q}^2 f_{B_q}^2 B_5^q; \end{aligned} \quad (28)$$

We then notice that the operator R_1^q defined in eq. (19) is trivially related to O_4^q ,

$$R_1^q = \frac{m_q}{m_b} O_4^q; \quad (29)$$

In addition, by using the Fierz identities and the equations of motion, the operator R_4^q can be expressed as [10]

$$2R_4^q = O_3^q + O_1^q + 2O_2^q - 2\frac{m_q}{m_b} O_5^q + R_2^q; \quad (30)$$

Thus, eqs. (29) and (30) can be used to get rid of the two parameters $B_{R_1}^q$ and $B_{R_4}^q$.

The values of the B -parameters obtained in ref. [13] and used in our calculation are collected in table 2. Concerning the unknown matrix elements of the operators R_2^q and R_3^q , they have been estimated in the VSA and we have included a 30% of relative error to account for the corresponding systematic uncertainty⁷.

In order to obtain the theoretical predictions presented in this paper, we have performed a Bayesian statistical analysis by implementing a simple Monte Carlo calculation. The input parameters have been extracted with flat distributions, by assuming the central values and standard deviations given in table 2.

4.1 Width differences: $\Delta\Gamma_d = \Delta\Gamma_d$, $\Delta\Gamma_s = \Delta\Gamma_s$ and $\Delta\Gamma_d = \Delta\Gamma_s$

The theoretical predictions for the width differences $\Delta\Gamma_d = \Delta\Gamma_d$ and $\Delta\Gamma_s = \Delta\Gamma_s$, as obtained from eq. (21) as functions of the CKM matrix elements and of the B -parameters entering at the

⁷Since terms proportional to $m_d=m_b$ are neglected in our calculation, the values of B_4^d and B_5^d are presented in the table only for completeness.

$m_b = 4.75 \quad 0.11 \text{ GeV}$ $\overline{m}_t(\overline{m}_t) = 165.0 \quad 5.0 \text{ GeV}$ $M_W = 80.41 \text{ GeV}$ $(B_s) = 1.461 \quad 0.057 \text{ ps}$ $M_{B_d} = 5.279 \text{ GeV}$ $\Gamma_b(\Gamma_b) = 0.85 \quad 0.02$	$m_c = m_b = 0.30 \quad 0.02$ $\overline{m}_s(\overline{m}_b) = 87 \quad 21 \text{ MeV}$ $\Gamma_d = 0.502 \quad 0.006 \text{ ps}^{-1}$ $(B_d) = 1.540 \quad 0.014 \text{ ps}$ $M_{B_s} = 5.369 \text{ GeV}$ $\Gamma_s(\Gamma_s) = 1.24 \quad 0.04$
$\Gamma_s(\Gamma_s) = 0.2240 \quad 0.0036$ $\Gamma_b(\Gamma_b) = 0.162 \quad 0.046$	$\Gamma_s(\Gamma_s) = 0.118$ $\Gamma_b(\Gamma_b) = 0.347 \quad 0.027$
$B_1^s = 0.87 \quad 0.05$ $B_2^s = 0.84 \quad 0.04$ $B_3^s = 0.91 \quad 0.08$ $B_4^s = 1.16 \quad 0.07$ $B_5^s = 1.75 \quad 0.20$	$B_1^s = B_1^d = 0.99 \quad 0.02$ $B_2^s = B_2^d = 1.01 \quad 0.02$ $B_3^s = B_3^d = 1.01 \quad 0.03$ $B_4^s = B_4^d = 1.01 \quad 0.02$ $B_5^s = B_5^d = 1.01 \quad 0.03$

Table 2: Central values and standard deviations of the input parameters used to obtain the theoretical estimates of the width differences and of the CP violation parameters. When the error is not quoted, the parameter has been kept fixed in the numerical analysis. The values of m_b and m_c refer to the pole masses, while \overline{m}_s and \overline{m}_t are the masses in the $\overline{\text{NDR}}\text{-}\overline{\text{MS}}$ scheme. The B -parameters are renormalized in the $\overline{\text{NDR}}\text{-}\overline{\text{MS}}$ scheme at the scale m_b . The definition of the renormalization scheme can be found in [11] for B_1^q , B_2^q and B_3^q and in [20] for B_4^q and B_5^q , see also appendix B.

LO in $1/m_b$, can be expressed as

$$\begin{aligned}
\frac{\Gamma_d}{\Gamma_s} &= 10^{-3} \left[0.96(10) + 5.48(34) \frac{B_2^d}{B_1^d} - 2.9(1.3) \frac{1}{B_1^d} \right. \\
&\quad \left. + \frac{\cos}{R_t} \left[0.80(13) + 0.24(7) \frac{B_2^d}{B_1^d} - 0.03(6) \frac{1}{B_1^d} \right] \right. \\
&\quad \left. + \frac{\cos 2}{R_t^2} \left[0.005(4) - 0.007(16) \frac{B_2^d}{B_1^d} - 0.008(17) \frac{1}{B_1^d} \right] \right]; \quad (31)
\end{aligned}$$

$$\frac{\Gamma_s}{\Gamma_b} = \frac{10^{-2}}{(R_t)^2} \left[0.02(2) + 0.77(7) \frac{B_2^s}{B_1^s} - 0.47(18) \frac{1}{B_1^s} \right]; \quad (32)$$

These formulae are one of the main results of this paper. In the above expressions, the terms proportional to $1/B_1^q$ represent the contributions of the $1/m_b$ corrections. Note also

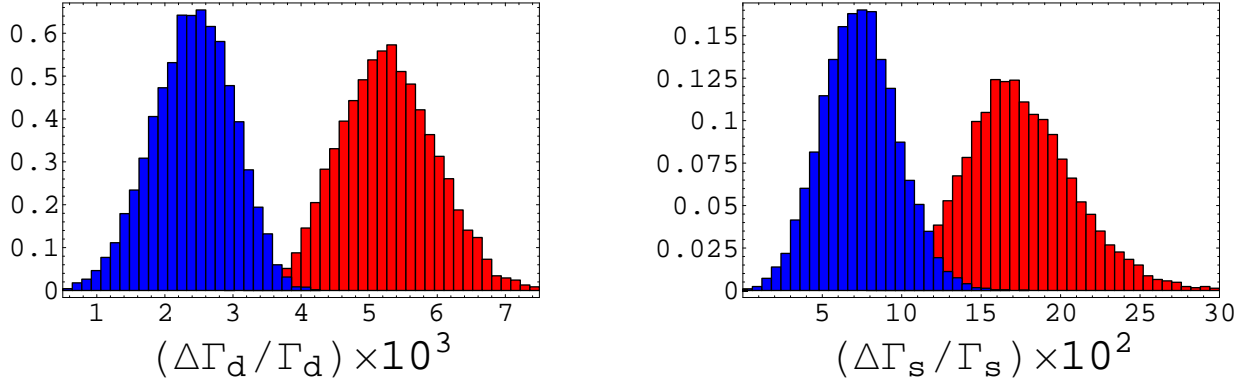


Figure 3: Theoretical distributions for the width differences in the B_d and B_s systems. The predictions are shown at both the LO (light/red) and NLO (dark/blue).

that, in order to obtain the prediction for $\Gamma_s = \Gamma_d$, the mass difference m_s has been evaluated in terms of m_d by using

$$m_s = m_d \frac{M_{B_s}}{M_{B_d}} \frac{V_{ts}^2}{V_{td}^2}; \quad (33)$$

where $\frac{V_{ts}^2}{V_{td}^2} = \frac{f_{B_s}^2}{f_{B_d}^2} \frac{B_1^s}{B_1^d}$.

The errors on the numerical coefficients presented in eqs. (31) and (32) take into account both the residual NNLO dependence on the renormalization scale of the $B = 1$ operators and the theoretical uncertainties on the various input parameters. To estimate the former, the scale μ_1 has been varied in the interval between $m_b = 2$ and $2m_b$. These errors are strongly correlated, since they originate from the theoretical uncertainties on the same set of input parameters. For this reason, they have not been used to derive our final predictions for the width differences. For these predictions, we quote the average and the standard deviation of the corresponding probability distribution functions obtained directly from the Monte Carlo simulation, namely

$$\Delta\Gamma_d = (2.42 \pm 0.59) \times 10^{-3}; \quad \Gamma_s = \Gamma_d = (7.4 \pm 2.4) \times 10^{-2}; \quad (34)$$

The theoretical distributions are shown in Fig. 3. Notice that the difference between the NLO and LO distributions is remarkable. The NLO corrections decrease the values of both $\Delta\Gamma_d$ and $\Gamma_s = \Gamma_d$ by about a factor two with respect to the LO predictions. We find that the total error on the width differences is dominated by the uncertainty on the b -quark mass in the first place, followed closely by the one due to the renormalization scale variation. Other contributions to the error, coming from the ratio $m_c = m_b$, the B - and the CKM-parameters are smaller, though not entirely negligible.

In Fig. 4 we show the dependence of $\Delta\Gamma_d$ on the mixing phase ϕ as given in eq. (31). NLO corrections in the limit of vanishing m_c just shift the LO curve, while m_c -dependent terms modify also its profile. In principle, a measurement of $\Delta\Gamma_d$ could allow a determination of ϕ , but we find that the dependence is so mild that the extracted value would be affected by a very large error.

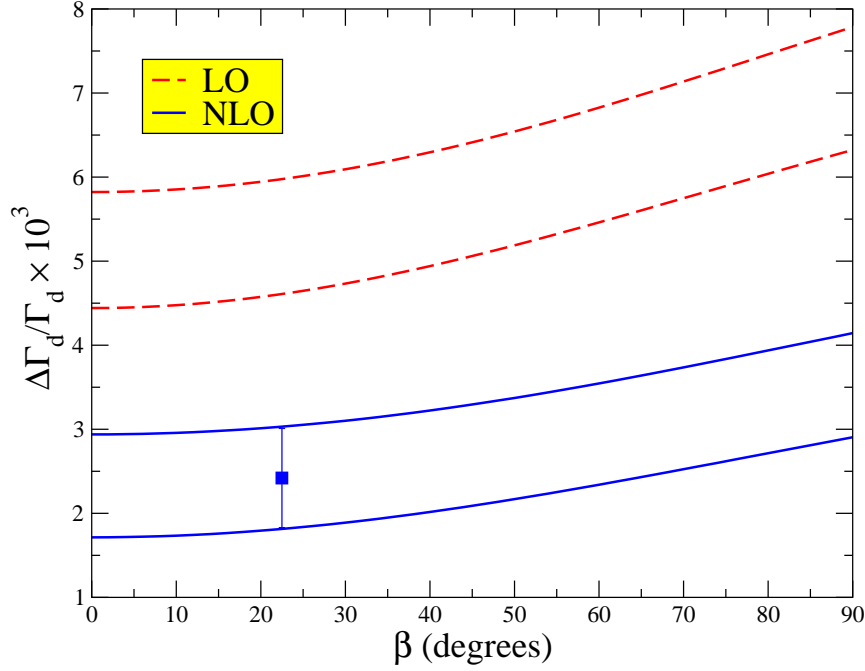


Figure 4: Prediction for $\Delta\Gamma_d/\Gamma_d$ as a function of β as obtained at the LO and NLO. The NLO estimate of $\Delta\Gamma_d/\Gamma_d$ at the measured value of β is also shown.

Another interesting prediction concerns the ratio $\Delta\Gamma_d/\Delta\Gamma_s$. This quantity is of particular interest, because the uncertainties coming from higher order QCD and α_s corrections, as well as those coming from the non-perturbative estimates of the B -parameters, are expected to cancel in this ratio to some extent. From our numerical analysis, we obtain the NLO prediction

$$\Delta\Gamma_d/\Delta\Gamma_s = (3.2 \pm 0.8) \times 10^{-2}. \quad (35)$$

The corresponding theoretical distributions at the LO and NLO are shown in Fig. 5. As can be seen from the plot, this quantity is practically unaffected by the NLO corrections.

4.2 CP Violation parameters: $j(q=p)_d$ and $j(q=p)_s$

CP violation in the mixing shows up only for a non-vanishing value of the charm quark mass, as can be explicitly verified from the expression of $j(q=p)_q$ in eq. (22). In addition, it is apparent from eq. (22) that $j(q=p)_s$ is suppressed with respect to $j(q=p)_d$ by a factor $\sin^2 \theta_s$.

For the parameters $j(q=p)_d$ and $j(q=p)_s$, expressed in terms of the CKM matrix elements and the B -parameters B_1^q, B_2^q , we obtain the expression

$$\frac{j(q=p)_d}{j(q=p)_s} = 10^{-4} \frac{\sin \theta_q}{R_{\text{eq}}} [5.19(84) + 1.57(47) \frac{B_2^q}{B_1^q} - 0.22(39) \frac{1}{B_1^q}]$$

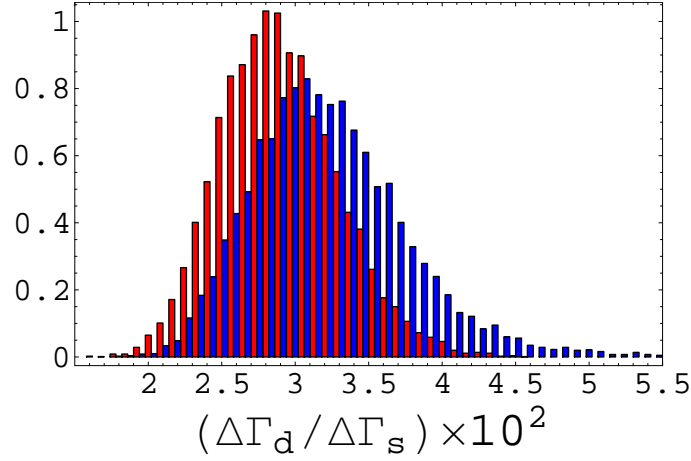


Figure 5: Theoretical distribution for the ratio $\Delta\Gamma_d/\Delta\Gamma_s$ as obtained at both the LO (light/red) and NLO (dark/blue).

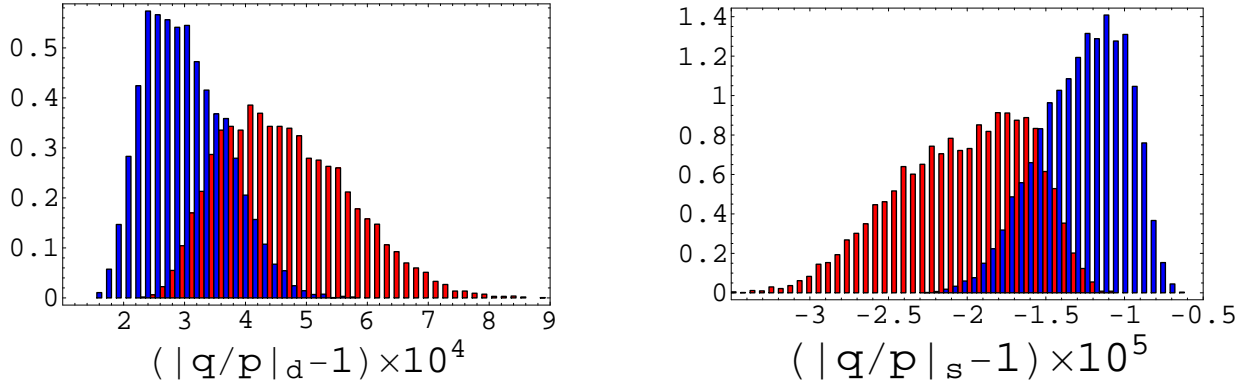


Figure 6: Theoretical distributions for $|q/p| - 1$ in the B_d and B_s systems. The predictions are shown at the LO (light/red) and NLO (dark/blue).

$$+ \frac{\sin 2\alpha_q}{R_{\text{eq}}^2} = 0.04(3) + 0.04(10) \frac{B_2^q}{B_1^q} + 0.05(11) \frac{1}{B_1^q} ; \quad (36)$$

where $q = d; s$.

By using the values of the CKM and B -parameters given in table 2 we obtain from the Monte Carlo analysis the final predictions

$$\frac{|q|}{p}_d - 1 = (2.96 \pm 0.67) \times 10^{-4} ; \quad \frac{|q|}{p}_s - 1 = (1.28 \pm 0.27) \times 10^{-5} ; \quad (37)$$

The theoretical distributions for these quantities are shown in Fig. 6 both at the LO and NLO. One can see that the effect of the NLO corrections turns out to be important also for these quantities. The error on $|q/p| - 1$ is largely dominated by the uncertainties on $m_c = m_b$ and on the CKM parameters. We note in particular that the dependence on

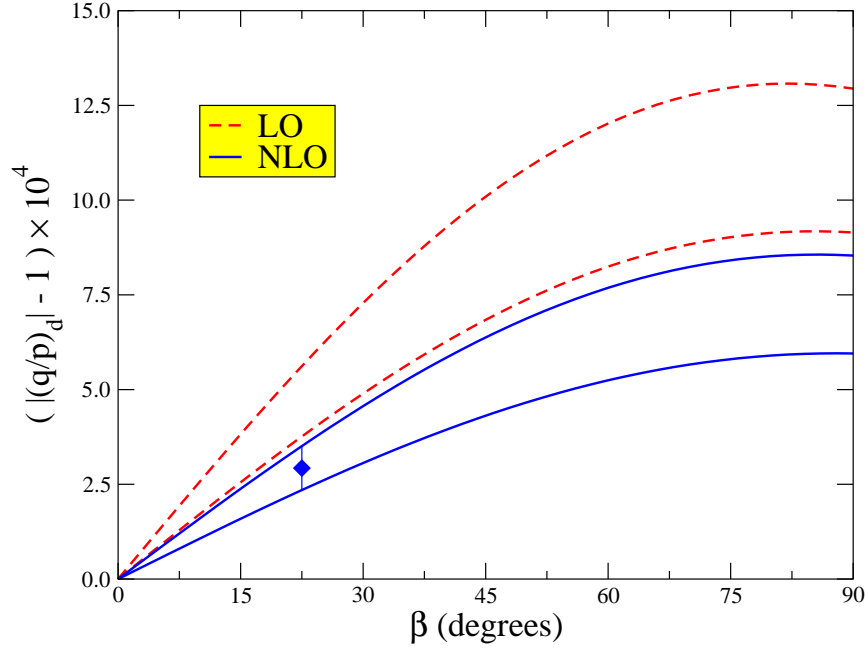


Figure 7: Prediction for the CP violation parameter $|j(q-p)_d| - 1$ as a function of β as obtained at both the LO and NLO. The NLO estimate of $|j(q-p)_d| - 1$ at the measured value of β is also shown.

the B parameters is practically negligible, making these predictions free from hadronic uncertainties.

Finally, we show in Fig. 7 the LO and NLO predictions for $|j(q-p)_d| - 1$ as functions of β . In this case, NLO corrections without charm mass leave the LO result practically unchanged, while the m_c -dependent terms give a sizable contribution. The dependence on β is quite strong, allowing for a determination of the mixing angle once $|j(q-p)_d| - 1$ will be measured.

5 Conclusions

The main result of this paper is the NLO QCD calculation of the Wilson coefficients entering the heavy quark expansion of Γ_{21}^d and Γ_{21}^s , including the effects of a non-vanishing charm quark mass. For Γ_{21}^s we find agreement with a previous result [11]. Using our results, we improve the theoretical predictions for different observables in the neutral B-meson systems, namely the width differences $\Gamma_d = \Gamma_d$ and $\Gamma_s = \Gamma_s$ and the CP violation parameters $|j(q-p)_d|$ and $|j(q-p)_s|$.

Using formulae including the NLO Γ_s corrections at the lowest order in the $1=m_b$ expansion and the first power corrections at the LO in Γ_s , we find

$$\frac{\Gamma_d}{\Gamma_d} = (2.42 \pm 0.59) \cdot 10^{-3}; \quad \frac{\Gamma_s}{\Gamma_s} = (7.4 \pm 2.4) \cdot 10^{-2}; \quad \frac{|j(q-p)_d|}{|j(q-p)_d|} = (3.2 \pm 0.8) \cdot 10^{-2};$$

$$j(q\bar{q})_d j^{-1} = (2.96 \pm 0.67) \cdot 10^{-4}; \quad j(q\bar{q})_s j^{-1} = (1.28 \pm 0.27) \cdot 10^{-5}; \quad (38)$$

NLO QCD corrections are in general important for theoretical consistency and give sizable contributions to the Wilson coefficients considered in this paper. We find that the charm quark mass effects at NLO are numerically important, in particular for $j(q\bar{q})_q j$ and should be included in the phenomenological analyses.

Acknowledgments

We thank D. Becirevic and J. Reyes for interesting discussions and suggestions on the subject of this paper. We also thank F. Martinez for correspondence on the experimental issues. Work partially supported by the European Community's Human Potential Programme under HPRN-CT-2000-00145 Hadrons/Lattice QCD.

Note added

Just before this paper was finalized, a paper by Beneke et al. on the same subject was submitted to the e-print archive [34]. Comparing the results, we found that the NLO contribution to the Wilson coefficients D_k^{cu} of eqs. (18) and (39) differ from the ones given in eq. (25) of ref. [34]. Had we assumed that the diagrams D_6, D_7 and D_8 in fig. 2 were equal to the corresponding "rotated" ones (i.e. those diagrams where the gluon is attached to the other external quark leg with the same flavour and to the other virtual quark line), we would have obtained the result of ref. [34]. However this assumption, which is correct when the two virtual lines correspond to the same flavour, does not hold when the two quarks are different. This may explain the origin of the discrepancy.

Appendix A: Analytical Results for the $B = 2$ Wilson Coefficients

In this appendix we collect the analytical expressions of the Wilson coefficients, both at the LO and NLO. The LO coefficients have been computed in refs. [10, 12] and are given here for completeness.

The coefficient functions D_k^{uu}, D_k^{cu} and D_k^{cc} defined in eq. (18) depend quadratically on the coefficient functions C_i of the $B = 1$ effective Hamiltonian and can be written as

$$\begin{aligned} D_k^{uu}(\mu) &= \sum_{i,j=1,2} C_i(\mu) C_j(\mu) F_{k,ij}^{uu}(\mu; \mu) + \frac{s}{4} C_2(\mu)^2 P_{k,22}^{uu}(\mu; \mu) \\ &\quad + 2 \frac{s}{4} C_2 C_{8G} P_{k,28}^u + 2 \sum_{i=1,2} \sum_{r=3,6} C_i C_r P_{k,ir}^u; \\ D_k^{cu}(\mu) &= \sum_{i,j=1,2} C_i(\mu) C_j(\mu) F_{k,ij}^{cu}(\mu; \mu) + \frac{s}{4} C_2(\mu)^2 P_{k,22}^{cu}(\mu; \mu) \\ &\quad + \frac{s}{4} C_2 C_{8G} (P_{k,28}^c + P_{k,28}^u) + \sum_{i=1,2} \sum_{r=3,6} C_i C_r (P_{k,ir}^c + P_{k,ir}^u); \end{aligned}$$

$$\begin{aligned}
D_k^{cc}(2) = & \sum_{i,j=1,2} C_i(1) C_j(1) F_{k,ij}^{cc}(1; 2) + \frac{s}{4} C_2(1)^2 P_{k,22}^{cc}(1; 2) \\
& + 2 \frac{s}{4} C_2 C_{8G} P_{k,28}^c + 2 \sum_{i=1,2} \sum_{r=3,6} C_i C_r P_{k,ir}^c :
\end{aligned} \quad (39)$$

The functions $F_{k,ij}^{qq^0}$ are obtained from the insertion of the operators Q_i and Q_j in the Feynman diagram SD_{11} of g. 2, whereas the diagram SD_{11} and D_{12} contribute to the functions $P_{k,22}^{qq^0}(1; 2)$ and $P_{k,ij}^q$ respectively. Contributions with the double insertion of penguin operators have been neglected, since the Wilson coefficients C_3, C_6 are numerically small.

We distinguish the leading and next-to-leading contributions in the coefficients $F_{k,ij}^{qq^0}$ by writing the expansion

$$F_{k,ij}^{qq^0} = A_{k,ij}^{qq^0} + \frac{s}{4} B_{k,ij}^{qq^0}; \quad (40)$$

where $(qq^0) = f(uu); (cu); (cc)g$. Since only the sum of $F_{k,12}^{qq^0}$ and $F_{k,21}^{qq^0}$ contributes to eq. (39), we just give in the following the average of the components 12 and 21. Moreover, we do not write explicitly the results for the functions D_k^{uu} since they can be obtained by taking the limit $m_c \rightarrow 0$ of D_k^{cc} .

In terms of the ratio $z = m_c^2/m_b^2$, the LO coefficients $A_{k,ij}^{qq^0}$ read

$$\begin{aligned}
A_{1,11}^{cu} &= \frac{3}{2} (2 - 3z + z^3); & A_{1,12}^{cu} &= A_{1,21}^{cu} = \frac{1}{2} (2 - 3z + z^3); & A_{1,22}^{cu} &= \frac{1}{2} (1 - z)^3; \\
A_{2,11}^{cu} &= 3 (1 - z)^2 (1 + 2z); & A_{2,12}^{cu} &= A_{2,21}^{cu} = (1 - z)^2 (1 + 2z); & A_{2,22}^{cu} &= (1 - z)^2 (1 + 2z);
\end{aligned} \quad (41)$$

$$\begin{aligned}
A_{1,11}^{cc} &= 3 \sqrt{1 - 4z} (1 - z); & A_{1,12}^{cc} &= \sqrt{1 - 4z} (1 - z); & A_{1,22}^{cc} &= \frac{1}{2} (1 - 4z)^{\frac{3}{2}}; \\
A_{2,11}^{cc} &= 3 \sqrt{1 - 4z} (1 + 2z); & A_{2,12}^{cc} &= \sqrt{1 - 4z} (1 + 2z); & A_{2,22}^{cc} &= \sqrt{1 - 4z} (1 + 2z);
\end{aligned} \quad (42)$$

The NLO results for the coefficients $B_{k,ij}^{qq^0}$ are presented in the $\overline{\text{MS}}$ scheme of ref. [21] for the $B = 1$ operators and the $\overline{\text{MS}}$ scheme of ref. [11] for the $B = 2$ operators, in QCD. We find

$$\begin{aligned}
B_{1,11}^{cu} &= \frac{109}{6} - 37z + \frac{3z^2}{2} + \frac{52z^3}{3} + 2(1 - z)^2 (5 + z) \log x_2 - 4(1 - z)^2 (5 + 7z) \log(1 - z) \\
&\quad - 2z \log z + 10 + 14z - 15z^2 \log z + 8(2 - 3z + z^3) \log(1 - z) \log z + 16(2 - 3z + z^3) L_{\frac{1}{2}}(z); \\
B_{2,11}^{cu} &= \frac{4}{3} (10 - 33z + 54z^2 - 31z^3 - 8(1 - z)^2 (4 + 14z - 3z^2) \log(1 - z) + \\
&\quad + 8z(2 - 23z + 21z^2 - 3z^3) \log z \\
&\quad + 16(1 - z)^2 (1 + 2z) (2 \log x_2 - \log(1 - z) \log z - 2L_{\frac{1}{2}}(z)));
\end{aligned} \quad (43)$$

$$\begin{aligned}
\frac{B_{1,12}^{cu} + B_{1,21}^{cu}}{2} &= \frac{502 + 912z - 387z^2 - 23z^3}{36} (1 - z)^2 (17 + 4z) \log x_1 + \frac{2}{3} (1 - z)^2 (5 + z) \log x_2 \\
&\quad + \frac{(1 - z)^2}{12z} (2 + 33z + 94z^2 - \log(1 - z)) - \frac{z}{12} (80 + 69z - 126z^2 - \log z +
\end{aligned}$$

$$\begin{aligned}
& \frac{8}{3} z^2 - 3z + z^3 (\log(1-z) \log z + 2\text{Li}_2(z)); \\
\frac{B_{2;12}^{\text{cu}} + B_{2;21}^{\text{cu}}}{2} = & \frac{130 + 93z + 144z^2 - 107z^3}{9} - \frac{2(1-z)^2}{3z} (1 + 15z + 47z^2 - 12z^3 \log(1-z) + \\
& \frac{2}{3} z - 8 - 93z + 87z^2 - 12z^3 \log z \\
& \frac{8}{3} (1-z)^2 (1+2z) (3 \log x_1 + 4 \log x_2 - 2 \log(1-z) \log z - 4\text{Li}_2(z)); \quad (44)
\end{aligned}$$

$$\begin{aligned}
B_{1;22}^{\text{cu}} = & \frac{2}{3} (1 - 5z + 4z^2) + \frac{136 - 159z + 738z^2 - 443z^3}{18} - 2(1-z)^2 (5 + 4z) \log x_1 + \\
& \frac{2}{3} (1-z)^2 (4-z) \log x_2 + \frac{(1-z)^2}{6z} (7 + 32z^2 + 3z^3 \log(1-z)) \\
& \frac{z}{6} (62 - 39z - 30z^2 + 3z^3 \log z) + \frac{5 - 3z - 18z^2 + 16z^3}{3} (\log(1-z) \log z + 2\text{Li}_2(z)); \\
B_{2;22}^{\text{cu}} = & \frac{8}{3} z^2 (1 + z - 2z^2) - \frac{28}{9} (5 + 3z - 27z^2 + 19z^3) - 16(1-z)^2 (1+2z) \log x_1 + \\
& \frac{32}{3} (1-z)^2 (1+2z) \log x_2 - \frac{4(1-z)^2}{3z} (1 - 12z - 16z^2 - 3z^3 \log(1-z) + \\
& \frac{4}{3} z - 2 - 3z + 18z^2 - 3z^3 \log z) + \frac{8}{3} (1 - 3z - 6z^2 + 8z^3) (\log(1-z) \log z + 2\text{Li}_2(z)); \quad (45)
\end{aligned}$$

$$\begin{aligned}
B_{1;11}^{\text{cc}} = & \frac{P \frac{1}{1-4z} - 109 - 226z + 168z^2}{6} - \frac{52 - 104z - 16z^2 + 56z^3 \log z}{6} + \\
& 2(5 - 8z) P \frac{1}{1-4z} \log x_2 - 12 P \frac{1}{1-4z} (3 - 2z) \log(1-4z) + 4(13 - 10z) P \frac{1}{1-4z} \log z + \\
& 16(1 - 3z + 2z^2 - 3 \log^2 z + 2 \log z \log(1-4z) - 3 \log z \log z + 4\text{Li}_2(z) + 2\text{Li}_2(z^2)); \\
B_{2;11}^{\text{cc}} = & \frac{8 P \frac{1}{1-4z} - 5 - 23z - 42z^2}{3} - \frac{16(4 - 2z - 7z^2 + 14z^3 \log z) - 32 P \frac{1}{1-4z} (1+2z) \log x_2}{3} \\
& - \frac{48 P \frac{1}{1-4z} (1+2z) \log(1-4z) + 64 P \frac{1}{1-4z} (1+2z) \log z}{3} + \\
& 16(1 - 4z^2 - 3 \log^2 z + 2 \log z \log(1-4z) - 3 \log z \log z + 4\text{Li}_2(z) + 2\text{Li}_2(z^2)); \quad (46)
\end{aligned}$$

$$\begin{aligned}
B_{1;12}^{\text{cc}} = & \frac{P \frac{1}{1-4z} - 127 - 199z - 75z^2}{9} + \frac{2(259z + 662z^2 - 76z^3 - 200z^4 \log z)}{12z} \\
& (17 - 26z) P \frac{1}{1-4z} \log x_1 + \frac{2(5 - 8z) P \frac{1}{1-4z} \log x_2}{3} - \frac{4 P \frac{1}{1-4z} (3 - 2z) \log(1-4z)}{3} \\
& \frac{P \frac{1}{1-4z} - 2 - 255z + 316z^2 \log z}{12z} + \\
& \frac{16(1 - 3z + 2z^2 - 3 \log^2 z + 2 \log z \log(1-4z) - 3 \log z \log z + 4\text{Li}_2(z) + 2\text{Li}_2(z^2))}{3}; \\
B_{2;12}^{\text{cc}} = & \frac{2 P \frac{1}{1-4z} - 68 + 49z - 150z^2}{9} + \frac{2(1 - 35z + 4z^2 + 76z^3 - 100z^4 \log z)}{3} + \\
& \frac{16(64z^2 \log^2 z - 8 P \frac{1}{1-4z} (1+2z) \log x_1 - \frac{32 P \frac{1}{1-4z} (1+2z) \log x_2}{3})}{3} \\
& \frac{16 P \frac{1}{1-4z} (1+2z) \log(1-4z) - \frac{2 P \frac{1}{1-4z} - 1 - 33z - 76z^2 \log z}{3z}}{3} + \\
& \frac{16(1 - 4z^2 - 2 \log z \log(1-4z) - 3 \log z \log z + 4\text{Li}_2(z) + 2\text{Li}_2(z^2))}{3}; \quad (47)
\end{aligned}$$

$$\begin{aligned}
B_{1;22}^{cc} &= \frac{2(1-10z)}{3} \frac{P \frac{1}{1-4z} (115+632z+96z^2)}{18} \frac{7+13z-194z^2+304z^3-64z^4 \log z}{6z} \\
&\quad + \frac{2 P \frac{1}{1-4z} (5-2z) \log x_1 + \frac{4(2-5z) P \frac{1}{1-4z} \log x_2}{18}}{4(1-6z) P \frac{1}{1-4z} \log(1-4z) +} \\
&\quad + \frac{13-54z+8z^2 \log \log(1-4z)}{3} + \frac{P \frac{3}{1-4z} (7+27z-250z^2 \log z)}{6z} + \\
&\quad + \frac{7-32z+4z^2 \log^2 \log \log z + \frac{4-5-12z+4z^2 \text{Li}_2(\cdot)}{3}}{3} + \frac{4-4-21z+2z^2 \text{Li}_2(\cdot^2)}{3}; \\
B_{2;22}^{cc} &= \frac{8-2(1+2z)}{3} \frac{8 P \frac{1}{1-4z} (19+53z+24z^2)}{9} + \frac{4(1+7z+10z^2-68z^3+32z^4 \log z)}{3z} \\
&\quad + \frac{8(1+2z)^2 \log^2 - 16 P \frac{1}{1-4z} (1+2z) \log x_1 + \frac{32 P \frac{1}{1-4z} (1+2z) \log x_2}{3}}{3} \\
&\quad + \frac{16 P \frac{1}{1-4z} (1+2z) \log(1-4z) - \frac{8(1+6z+8z^2 \log \log(1-4z))}{3}}{3} \\
&\quad + \frac{4 P \frac{1}{1-4z} (1+9z+26z^2 \log z)}{3z} + 8(1+2z)^2 \log \log z + \\
&\quad + \frac{32(1-4z^2 \text{Li}_2(\cdot))}{3} - \frac{32(1+3z+2z^2 \text{Li}_2(\cdot^2))}{3}; \tag{48}
\end{aligned}$$

where ρ is the ratio

$$\rho = \frac{1}{1 + \frac{P \frac{1}{1-4z}}{P \frac{1}{1-4z}}}; \tag{49}$$

and we have defined $x_1 = 1-m_b$ and $x_2 = 2-m_b$.

The contributions of the diagram D_{11} in Fig. 2 and of the insertions of the penguin and chromomagnetic operators, read

$$\begin{aligned}
P_{1;22}^{cu} &= \frac{1}{27} \frac{2z}{9} \frac{\log x_1}{9} \frac{P \frac{1}{1-4z} (1+2z) (2+3 \log \rho + 6 \log x_1)}{54} + \frac{\log z}{18}; \\
P_{2;22}^{cu} &= \frac{8}{27} + \frac{16z}{9} + \frac{8 \log x_1}{9} + \frac{4 P \frac{1}{1-4z} (1+2z) (2+3 \log \rho + 6 \log x_1)}{27} - \frac{4 \log z}{9}; \tag{50}
\end{aligned}$$

$$\begin{aligned}
P_{1;22}^{cc} &= \frac{2 P \frac{1}{1-4z} (1+8z+12z^2)}{27} \frac{\log}{9} + \frac{4z^2 \log}{3} + \frac{16z^3 \log}{9} \\
&\quad + \frac{P \frac{1}{1-4z} (1+2z) (2 \log x_1 - \log z)}{9}; \\
P_{2;22}^{cc} &= \frac{16 P \frac{1}{1-4z} (1+8z+12z^2)}{27} + \frac{8 \log}{9} - \frac{32z^2 \log}{3} - \frac{128z^3 \log}{9} + \\
&\quad + \frac{8 P \frac{1}{1-4z} (1+2z) (2 \log x_1 - \log z)}{9}; \tag{51}
\end{aligned}$$

$$\begin{aligned}
P_{1;13}^c &= 3 P \frac{1}{1-4z} (1-z); & P_{1;23}^c &= P \frac{1}{1-4z} (1-z); & P_{1;14}^c &= P \frac{1}{1-4z} (1-z); \\
P_{2;13}^c &= 3 P \frac{1}{1-4z} (1+2z); & P_{2;23}^c &= P \frac{1}{1-4z} (1+2z); & P_{2;14}^c &= P \frac{1}{1-4z} (1+2z); \tag{52}
\end{aligned}$$

$$\begin{aligned}
P_{1;24}^c &= \frac{1}{2} P \frac{(1-4z)^{\frac{3}{2}}}{1-4z} (1+2z); & P_{1;15}^c &= 9z P \frac{1}{1-4z}; & P_{1;25}^c &= 3z P \frac{1}{1-4z}; \\
P_{2;24}^c &= P \frac{1}{1-4z} (1+2z); & P_{2;15}^c &= 0; & P_{2;25}^c &= 0; \tag{53}
\end{aligned}$$

$$\begin{aligned}
P_{1;16}^c &= 3z P \frac{1}{1-4z}; & P_{1;26}^c &= 3z P \frac{1}{1-4z}; & P_{1;28}^c &= \frac{1}{3} P \frac{1}{1-4z} (1+2z); \\
P_{2;16}^c &= 0; & P_{2;26}^c &= 0; & P_{2;28}^c &= \frac{4}{3} P \frac{1}{1-4z} (1+2z); \tag{54}
\end{aligned}$$

The functions $P_{k;ij}^u$ can be obtained from $P_{k;ij}^c$ by taking the limit $z \rightarrow 0$.

Appendix B : Evanescent Operators and Renormalization Schemes

In this appendix, we define the $\overline{\text{NDR-MS}}$ scheme chosen to renormalize the QCD, $B = 2$ operators whose Wilson coefficients are given in appendix A. This scheme is introduced in ref. [11] by giving three prescriptions (eqs. (13)–(15) of that paper) which define implicitly the relevant evanescent operators. In order to make it more explicit, we write out in this appendix the complete basis of operators and evanescent operators defining this scheme. Although this renormalization scheme is the only one needed to define our results, we think it may be useful, for future applications, to present also the matching matrix which relates the QCD operators in the $\overline{\text{NDR-MS}}$ of [11] to a corresponding set of HQET operators. This matrix has been computed and used in the intermediate steps of our calculation. To this purpose, we consider a $\overline{\text{NDR-MS}}$ scheme for the HQET operators which is a simple generalization of the one defined in ref. [22]. In addition, since a second $\overline{\text{NDR-MS}}$ renormalization scheme has been introduced in ref. [21] for the $B = 2$ operators in QCD, we also discuss this scheme and present the corresponding NLO matching matrix relating the QCD operators to the HQET ones.

To start with, we introduce the following set of $B = 2$ four-fermion operators,

$$\begin{aligned} O_1^q &= (\bar{b}_i q_i)_{V-A} (\bar{b}_j q_j)_{V-A} ; & O_2^q &= (\bar{b}_i q_i)_{S-P} (\bar{b}_j q_j)_{S-P} ; \\ O_3^q &= (\bar{b}_i \not{L} q_i) (\bar{b}_j \not{L} q_j) ; & O_4^q &= (\bar{b}_i q_j)_{S-P} (\bar{b}_j q_i)_{S-P} ; \end{aligned} \quad (55)$$

where, for any string of Dirac matrices, we define $\not{L} = (1 - \gamma_5)$.

Concerning the evanescent operators, it is worth to recall that they are renormalized, in any given renormalization scheme, in such a way that their matrix elements vanish on IR finite, physical external states. Consequently, the anomalous dimension matrix elements mixing the physical and the evanescent operators vanish to all orders [33]. Furthermore, while the evanescent operators usually only enter the definition of the renormalization scheme, in some cases they can also contribute beyond the LO to the matching of the physical operators. In particular, when the matching is performed in the presence of IR divergences, as in our calculation, one should properly take into account the contribution of the matrix elements of the evanescent operators to the matching conditions of the physical operators [6, 20].

We now proceed by defining in details the several renormalization schemes discussed above.

$\overline{\text{NDR-MS}}$ scheme for QCD operators of ref. [11]

This scheme concerns $B = 2$ operators in QCD. The four-dimensional basis involves the operators O_1^q, O_2^q and O_4^q in eq. (55), whereas the evanescent operators are

$$\begin{aligned} S_1^q &= (\bar{b}_i q_j)_{V-A} (\bar{b}_j q_i)_{V-A} - O_1^q ; \\ S_2^q &= (\bar{b}_i \not{L} q_j) (\bar{b}_j \not{L} q_i) - (16 - 4'') (S_1^q + O_1^q) ; \end{aligned}$$

$$\begin{aligned}
S_3^q &= (\bar{b}_i \gamma_\mu \gamma_5 q_j) (\bar{b}_j \gamma_\mu \gamma_5 q_i) - (4 - 2\epsilon) O_4^q - (8 - 8\epsilon) O_2^q; \\
S_4^q &= (\bar{b}_i \gamma_\mu \gamma_5 q_j) (\bar{b}_j \gamma_\mu \gamma_5 q_j) - (16 - 4\epsilon) O_1^q; \\
S_5^q &= (\bar{b}_i \gamma_\mu \gamma_5 q_i) (\bar{b}_j \gamma_\mu \gamma_5 q_j) - (4 - 2\epsilon) O_2^q - (8 - 8\epsilon) O_4^q;
\end{aligned} \tag{56}$$

$\overline{\text{MS}}$ scheme for QCD operators of ref. [21]

This scheme is defined by choosing O_1^q, O_2^q and O_3^q in eq. (55) as operators of the physical basis and the following set of evanescent operators

$$\begin{aligned}
M_1^q &= (\bar{b}_i q_j)_{V-A} (\bar{b}_j q_i)_{V-A} - O_1^q; \\
M_2^q &= (\bar{b}_i \gamma_\mu \gamma_5 q_j) (\bar{b}_j \gamma_\mu \gamma_5 q_i) - (16 - 4\epsilon) (M_1^q + O_1^q); \\
M_3^q &= (\bar{b}_i \gamma_\mu \gamma_5 q_j) (\bar{b}_j \gamma_\mu \gamma_5 q_i) - 6O_2^q - O_3^q = 2; \\
M_4^q &= (\bar{b}_i q_j)_{S-P} (\bar{b}_j q_i)_{S-P} + O_2^q = 2 - O_3^q = 8; \\
M_5^q &= (\bar{b}_i \gamma_\mu \gamma_5 q_j) (\bar{b}_j \gamma_\mu \gamma_5 q_i) - 16M_3^q - 64M_4^q - 64O_2^q - 16(1 - \epsilon) O_3^q; \\
M_6^q &= (\bar{b}_i \gamma_\mu \gamma_5 q_i) (\bar{b}_j \gamma_\mu \gamma_5 q_j) - (16 - 4\epsilon) O_1^q; \\
M_7^q &= (\bar{b}_i \gamma_\mu \gamma_5 q_i) (\bar{b}_j \gamma_\mu \gamma_5 q_j) - (64 - 96\epsilon) O_2^q - (16 - 8\epsilon) O_3^q;
\end{aligned} \tag{57}$$

$\overline{\text{MS}}$ scheme for HQET operators

In the $B = 2$ HQET Hamiltonian, we choose the operators O_1^q and O_2^q in eq. (55) as operators of the physical basis and the following set of evanescent operators,

$$\begin{aligned}
H_1^q &= (\bar{b}_i q_j)_{V-A} (\bar{b}_j q_i)_{V-A} - O_1^q \\
H_2^q &= (\bar{b}_i \gamma_\mu \gamma_5 q_j) (\bar{b}_j \gamma_\mu \gamma_5 q_i) - (16 - 4\epsilon) (H_1^q + O_1^q) \\
H_3^q &= (\bar{b}_i \gamma_\mu \gamma_5 q_j) (\bar{b}_j \gamma_\mu \gamma_5 q_i) + (4 - 2\epsilon) (H_1^q + O_1^q) + (4 - 2\epsilon) (H_4^q - O_1^q = 2 - O_2^q) \\
H_4^q &= O_4^q + O_1^q = 2 + O_2^q \\
H_5^q &= (\bar{b}_i \gamma_\mu \gamma_5 q_i) (\bar{b}_j \gamma_\mu \gamma_5 q_j) - (16 - 4\epsilon) O_1^q \\
H_6^q &= O_3^q + (4 - 2\epsilon) O_1^q + (4 - 2\epsilon) O_2^q
\end{aligned} \tag{58}$$

where O_3^q and O_4^q are also defined in eq. (55). The parameters ϵ and γ_5 are not fixed and enter the definition of the renormalization scheme. For the specific choice $\epsilon = 0$ this scheme reduces to the one considered in ref. [22]. In four dimensions the operators $H_1^q - H_6^q$ vanish because of the Fierz identities, the Chisholm identity

$$\gamma_\mu \gamma_5 \gamma_\nu = g_{\mu\nu} + i\epsilon_{\mu\nu\alpha\beta} \gamma_\alpha \gamma_\beta \gamma_5 \tag{59}$$

and the equation $\gamma_5^2 = 1$, verified by the γ_5 -eld operator in the static limit. Notice that, since H_4^q and H_6^q are evanescent, both O_3^q and O_4^q in the HQET are reducible in terms of O_1^q and O_2^q and need not to be included in the basis.

Matching between QCD and HQET operators

We now discuss the matching, at the NLO, between QCD and HQET operators. The matching condition can be written as

$$O_k(m_b)_{\text{QCD}} = C_{k1} O_1(m_b)_{\text{HQET}} + O(1/m_b); \tag{60}$$

where a common renormalization scale $\mu = m_b$ has been chosen. Let us stress that the equation above is only valid once the operators are sandwiched between external on-shell states.

For the QCD NDR- \overline{MS} scheme of ref. [11], the matrix \mathcal{C} has been given at $\mathcal{O}(\alpha_s)$ in ref. [13], by considering in the HQET the renormalization scheme defined above with the particular choice $\mu = m_b = 0$. We have repeated the calculation for generic μ and m_b and obtained

$$\begin{pmatrix} 0 & 1 \\ \text{B} & \text{C} \end{pmatrix} \begin{pmatrix} O_1(m_b) \\ O_2(m_b) \\ O_4(m_b) \end{pmatrix}_{\text{QCD}} \stackrel{1 \text{ ref: [11]}}{=} \begin{pmatrix} 20 & 1 & 0 \\ 6 & 0 & 1 \\ 4 & 1 & 1 \end{pmatrix} \begin{pmatrix} 1 \\ \text{C} \\ \text{A} \end{pmatrix} + \frac{s(m_b)}{4} D_1 \begin{pmatrix} 3 \\ 7 \\ 15 \end{pmatrix} \begin{pmatrix} O_1(m_b) \\ O_2(m_b) \end{pmatrix}_{\text{HQET}}; \quad (61)$$

$$D_1 = \begin{pmatrix} 0 & 1 \\ \text{B} & \text{C} \end{pmatrix} : \begin{pmatrix} 14 & 8 \\ \frac{39}{24} \frac{3+4}{121+3} & \frac{25}{3} \frac{11+4}{11+3} \end{pmatrix} \begin{pmatrix} 1 \\ \text{C} \\ \text{A} \end{pmatrix}; \quad (62)$$

For $\mu = m_b = 0$ this confirms the previous results.

Notice that in QCD the operator O_4^q is in general independent from the operators O_1^q and O_2^q . However, its matrix elements between external on-shell states can be expressed in terms of the matrix elements of O_1^q and O_2^q . This relation has been given in ref. [11] in terms of the operator

$$R_0^q = O_4^q + O_1^q = 2 + O_2^q; \quad (63)$$

The on-shell matrix elements of R_0^q are of short-distance origin and their values can be easily obtained by using the matching coefficients between QCD and HQET operators given in eq. (61).

When the QCD operators are renormalized in the NDR- \overline{MS} of ref. [21] the matrix \mathcal{C} is given by

$$\begin{pmatrix} 0 & 1 \\ \text{B} & \text{C} \end{pmatrix} \begin{pmatrix} O_1(m_b) \\ O_2(m_b) \\ O_3(m_b) \end{pmatrix}_{\text{QCD}} \stackrel{1 \text{ ref: [21]}}{=} \begin{pmatrix} 20 & 1 & 0 \\ 6 & 0 & 1 \\ 4 & 1 & 1 \end{pmatrix} \begin{pmatrix} 1 \\ \text{C} \\ \text{A} \end{pmatrix} + \frac{s(m_b)}{4} D_1 \begin{pmatrix} 3 \\ 7 \\ 15 \end{pmatrix} \begin{pmatrix} O_1(m_b) \\ O_2(m_b) \end{pmatrix}_{\text{HQET}}; \quad (64)$$

$$D_1 = \begin{pmatrix} 0 & 1 \\ \text{B} & \text{C} \end{pmatrix} : \begin{pmatrix} 14 & 8 \\ \frac{35}{24} \frac{3+4}{237+3} & \frac{13}{3} \frac{27+4}{27+3} \end{pmatrix} \begin{pmatrix} 1 \\ \text{C} \\ \text{A} \end{pmatrix}; \quad (65)$$

By using the above results one also finds that in this scheme the matching of the operator O_4 onto the HQET operators is given by

$$(O_4(m_b))_{QCD}^{\text{ref: [21]}} = \left(1 - \frac{1}{2} \right) + \frac{s(m_b)}{4} \left(\frac{101 + 3}{24} - \frac{4}{3} \right) \frac{7}{3} \frac{O_1(m_b)}{O_2(m_b)}_{HQET} : \quad (66)$$

References

- [1] M. Battaglia et al., arXiv:hep-ph/0304132.
See also The Heavy Flavor Averaging Group (HFAG), <http://www.slac.stanford.edu/xorg/hfag/>
- [2] B. Aubert et al. [BABAR Collaboration], arXiv:hep-ex/0303043.
- [3] M. Ciuchini, E. Franco, F. Parodi, V. Lubicz, L. Silvestrini and A. Stocchi, arXiv:hep-ph/0307195.
- [4] V. A. Khoze, M. A. Shifman, N. G. Uraltsev and M. B. Voloshin, Sov. J. Nucl. Phys. 46 (1987) 112 [Yad. Fiz. 46 (1987) 181].
- [5] J. Chay, H. Georgi and B. Grinstein, Phys. Lett. B 247 (1990) 399.
- [6] M. Ciuchini, E. Franco, V. Lubicz and F. Mescia, Nucl. Phys. B 625, 211 (2002) [hep-ph/0110375].
- [7] M. Beneke, G. Buchalla, C. Greub, A. Lenz and U. Nierste, Nucl. Phys. B 639, 389 (2002) [hep-ph/0202106].
- [8] E. Franco, V. Lubicz, F. Mescia and C. Tarantino, Nucl. Phys. B 633, 212 (2002) [hep-ph/0203089].
- [9] F. Gabbiani, A. I. Onishchenko and A. A. Petrov, arXiv:hep-ph/0303235.
- [10] M. Beneke, G. Buchalla and I. Dunietz, Phys. Rev. D 54, 4419 (1996) [hep-ph/9605259].
- [11] M. Beneke, G. Buchalla, C. Greub, A. Lenz and U. Nierste, Phys. Lett. B 459, 631 (1999) [hep-ph/9808385].
- [12] A. S. Dighe, T. Hurth, C. S. Kim and T. Yoshikawa, Nucl. Phys. B 624, 377 (2002) [hep-ph/0109088].
- [13] D. Becirevic, V. Ginzburg, G. Martinelli, M. Papinutto and J. Reyes, JHEP 0204, 025 (2002) [hep-lat/0110091].
- [14] J. S. Hagelin, Nucl. Phys. B 193, 123 (1981).
- [15] A. J. Buras, M. Jamnitsch and P. H. Weisz, Nucl. Phys. B 347, 491 (1990).
- [16] A. J. Buras, M. Jamnitsch, M. E. Lautenbacher and P. H. Weisz, Nucl. Phys. B 400 (1993) 37 [hep-ph/9211304].

- [17] A .J. Buras, M . Jam in and M .E. Lautenbacher, Nucl. Phys. B 400 (1993) 75 [[hep-ph/9211321](#)].
- [18] M . Ciuchini, E . Franco, G . Martinelli and L . Reina, Nucl. Phys. B 415 (1994) 403 [[hep-ph/9304257](#)].
- [19] R . Mertig and R . Scharf, Comput. Phys. Commun. 111 (1998) 265 [[hep-ph/9801383](#)].
- [20] M . Misiak and J . Urban, Phys. Lett. B 451 (1999) 161 [[hep-ph/9901278](#)].
- [21] A .J. Buras, M . Misiak and J . Urban, Nucl. Phys. B 586, 397 (2000) [[hep-ph/0005183](#)].
- [22] V . Gimenez and J . Reyes, Nucl. Phys. B 545 (1999) 576 [[arXiv:hep-lat/9806023](#)].
- [23] V . Gimenez and J . Reyes, Nucl. Phys. Proc. Suppl. 94 (2001) 350 [[hep-lat/0010048](#)].
- [24] S . Hashimoto, K . I. Ishikawa, T . Onogi, M . Sakamoto, N . Tsutsui and N . Yamada, Phys. Rev. D 62 (2000) 114502 [[hep-lat/0004022](#)].
- [25] S . Aoki et al. [JLQCD Collaboration], Phys. Rev. D 67 (2003) 014506 [[hep-lat/0208038](#)].
- [26] D . Becirevic, D . Mebni, A . Retico, V . Gimenez, V . Lubicz and G . Martinelli, Eur. Phys. J. C 18 (2000) 157 [[hep-ph/0006135](#)].
- [27] L . Leblond and C . J. Lin [UKQCD Collaboration], Phys. Rev. D 64 (2001) 094501 [[hep-ph/0011086](#)].
- [28] N . Yamada et al. [JLQCD Collaboration], Nucl. Phys. Proc. Suppl. 106 (2002) 397 [[hep-lat/0110087](#)].
- [29] S . Aoki et al. [JLQCD Collaboration], [arXiv:hep-ph/0307039](#).
- [30] J . G . Komer, A . I. Onishchenko, A . A . Petrov and A . A . Pivovarov, [arXiv:hep-ph/0306032](#).
- [31] K . Hagiwara, S . Narison and D . Nomura, Phys. Lett. B 540, 233 (2002) [[hep-ph/0205092](#)].
- [32] S . Narison and A . A . Pivovarov, Phys. Lett. B 327, 341 (1994) [[hep-ph/9403225](#)].
- [33] M . J. Dugan and B . Grinstein, Phys. Lett. B 256 (1991) 239.
- [34] M . Beneke, G . Buchalla, A . Lenz and U . Nierste, [arXiv:hep-ph/0307344](#).